Internal Report
DESY F41-76/11
December 1976

Basic Properties of Synchrotron Radiation

by

R. Haensel and G. Zimmerer

BASIC PROPERTIES OF SYNCHROTRON RADIATION

by

R. Haensel
Institut für Experimentalphysik der Universität Kiel, 2300 Kiel,

and

G. Zimmerer
II. Institut für Experimentalphysik der Universität Hamburg,
2000 Hamburg 50, Fed. Rep. Germany

1. HISTORICAL REMARKS

As has been recently pointed out by Baldwin [1] the "discovery of synchrotron radiation is an interesting case history in the nature of scientific discovery". When the first betatrons were built during World War II the role of radiation losses in these machines was considered. In principle, from classical electrodynamics, it was well known that each accelerated electrically charged particle radiates. An expression for the instantaneous total power radiated by a single, non relativistic electron was given by Larmor [2] at the end of the last century as

$$P = \frac{2}{3}\cdot\frac{e^2}{c^3}\cdot\left|\frac{d\vec{v}}{dt}\right|^2 = \frac{2}{3}\cdot\frac{e^2}{m^2c^3}\cdot\left|\frac{d\vec{p}}{dt}\right|^2 \qquad (1.1)$$

where e is the electric charge, c is the velocity of light, $\vec{v}$ and $\vec{p}$ are the velocity and momentum, respectively, of the charged particle, m is its rest mass. Liénard [3] developed a generalization of the Larmor equation showing that an electron moving in a circular orbit would become a source of intense electromagnetic radiation because of its strong centripetal acceleration. Schott [4] has used this theory in an attempt to explain the discrete nature of atomic spectra. His result of a continuous radiation loss of the atomic electrons was in obvious contrast to the experimental facts. The explanation of the discrete atomic spectra lateron came from Bohr who developed the theory of stationary energy states of the atom.

Since radiation losses were generally expected but not experimentally observed in the first betatrons the subject was forgotten until Ivanenko and Pomeranchuk [5] pointed out that radiation losses would cause an upper limit for the maximum energy obtainable with a betatron. The first systematic search for the radiation in the General Electric Laboratories at Schenectady, N.Y., by Blewett [6] had no clear results. Only a shrinking of the electron orbit at the highest energy of a 100 MeV betatron was observed [6] which was in qualitative accordance with the results of Ivanenko and Pomeranchuk [5]. However, an alternative explanation could also have been responsible for these observations [1].

Three years later, a new 70 MeV electron synchrotron was built in the same laboratory. In this machine, an assistant of Pollock et al [7], Floyd Haber, for the first time visually observed the radiation as an intense "arc" [1]. The radiation got its name "synchrotron radiation" (SR) because it was found experimentally from an electron synchrotron. Nevertheless it is sometimes called betatron-, cyclotron radiation or magnetic bremsstrahlung.

The discovery of SR led to systematic investigations of its characteristics, both from the theoretical and experimental point of view. Ivanenko, Sokolov et al [8-13] in Moscow have made the first and most extensive theoretical studies, both classically and quantum mechanically. In close connection with the experiments at General Electric, Schwinger [14-16] independently derived the theory and came to equations directly applicable for the work at accelerators. Other theoretical work was done by Olsen [17] and Neumann [18]. A comparison of the classical and quantum mechanical approach shows agreement within error bars, which are negligible for the presently available accelerators.

Systematic experimental studies have been made by Elder et al [19] at the General Electric synchrotron. Ado and Cherenkov [20] and Korolev et al [21,22] not only investigated the characteristics of SR but also its interaction with the electron beam itself at the 250 MeV synchrotron of the Lebedev Institute in Moscow. At the 300 MeV synchrotron at Cornell, Corson [23] observed the shrinking of the electron orbit and proved the "E^4-law". At the same accelerator, Tomboulian et al [24-26] measured the spectral characteristics, and Joos [27] and Bedo et al [28] the polarization of SR. Systematic studies have also been performed at the NBS 180 MeV synchrotron by Madden and Codling [29-31], and by Bathow et al [32] at the 6 GeV synchrotron in Hamburg.

Tomboulian [24,25] was the first to point out that SR would be a very interesting VUV light source because of its outstanding properties. Unfortunately he himself had no opportunity to use the

Cornell synchrotron for spectroscopic purposes on a large scale but his idea was picked up by others. In the last 20 years a great number of high energy particle accelerators and storage rings have been partially or exclusively used as SR-sources. Specific aspects of studies with SR have been covered by a number of review papers [33-42], conference proceedings [43-46] and a bibliographical compilation [47].

2. QUALITATIVE DESCRIPTION OF SR CHARACTERISTICS

2.1 Total power

2.1.1 General case. The Larmor formula (Eq. 1.1) gives the instantaneous power, P, radiated by an accelerated non relativistic electron into the full solid angle. The situation is drastically changed when the velocity of the electron more and more approaches the velocity of light ($\beta = v/c \approx 1$). Now the Lorentz-invariant form of Eq. 1.1 must be used [48]. Because electromagnetic energy, E_{rad}, and elapsed time, t, transform in the same manner under Lorentz transformations, the instantaneous power is already an invariant ($dE_{rad} = Pdt$). The Lorentz invariant right hand side of Eq. 1.1 is found by first replacing the time derivative by the derivative with respect to the invariant proper time, τ. The differential of proper time is defined by

$$d\tau = \gamma^{-1} \cdot dt \qquad (2.1.1)$$

with

$$\gamma = \frac{E}{mc^2} = (1-\beta^2)^{-1/2} \qquad (2.1.2)$$

E is the total energy of the relativistic electron, m its rest mass.

Secondly, we have to replace the momentum of the electron by its momentum-energy 4-vector.

$$\left(\frac{dp}{d\tau}\right)^2 \Longrightarrow \left(\frac{dp}{d\tau}\right)^2 - \frac{1}{c^2} \cdot \left(\frac{dE}{d\tau}\right)^2 \qquad (2.1.3)$$

In this way we obtain the following form of Eq. 1.1

$$P = \frac{2e^2}{3m^2c^3} \cdot \left[\left(\frac{dp}{d\tau}\right)^2 - \frac{1}{c^2} \cdot \left(\frac{dE}{d\tau}\right)^2\right]$$

$$= \frac{2e^2}{3m^2c^3} \cdot \gamma^2 \cdot \left[\left(\frac{dp}{dt}\right)^2 - \frac{1}{c^2}\left(\frac{dE}{dt}\right)^2\right] \qquad (2.1.4)$$

Another form of Eq. 2.1.4 can be obtained by writing $\vec{p} = \gamma m \cdot \vec{v}$, $E = \gamma mc^2$. Performing the indicated differentiations we obtain

$$P = \frac{2}{3}\,\frac{e^2}{c^3} \cdot \gamma^6 \cdot \left[\left(\frac{d\vec{v}}{dt}\right)^2 - \left(\frac{\vec{v}}{c} \times \frac{d\vec{v}}{dt}\right)^2\right] \qquad (2.1.5)$$

There are two important special cases which must be considered:

(i) Linear acceleration ($d\vec{v}/dt$ parallel to $\vec{v}$)

(ii) Circular acceleration ($d\vec{v}/dt$ perpendicular to $\vec{v}$)

2.1.2 Linear acceleration. From $E^2 = p^2c^2 + (mc^2)^2$, we calculate the relation between the change in momentum and the change in energy.

$$c^2 \cdot p \cdot \left(\frac{dp}{dt}\right) = E \cdot \left(\frac{dE}{dt}\right) \qquad (2.1.6)$$

Therefore, Eq. 2.1.4 is reduced to

$$P = \frac{2}{3}\,\frac{e^2}{m^2c^3}\left(\frac{dp}{dt}\right)^2 = \frac{2}{3}\,\frac{e^2}{m^2c^3}\left(\frac{dE}{dx}\right)^2 \qquad (2.1.7)$$

(the particle may move in x-direction)

For linear acceleration the radiated power does not depend on the total energy of the particle but only on its change.

We compare the instantaneous power radiated by an electron and the rate of change of its total energy in the case of linear acceleration:

$$\frac{P}{dE/dt} = \frac{2}{3}\,\frac{e^2}{m^2c^3} \cdot \frac{(dE/dx)^2}{v \cdot (dE/dx)}$$

$$\approx \frac{2}{3}\,\frac{e^2/mc^2}{mc^2} \cdot \frac{dE}{dx} \qquad (v \approx c) \qquad (2.1.8)$$

Eq. 2.1.8 shows that radiation losses in linear accelerators will be negligible unless the gain in energy along a distance e^2/mc^2 = classical electron radius is comparable to the rest energy, mc^2, of the particle. For electrons, e.g., the energy gain must be of the order of 1.8×10^{14} MeV/m unless the radiation losses get the limiting factor for the accelerator. Typical values which can be realized today are ~10 MeV/m (see, e.g. the numbers of SLAC: length of the linear accelerator 3000 m, final energy of the electrons ~20 GeV).

2.1.3 Circular acceleration. In a circular accelerator the situation is drastically different. As long as the energy loss of the particle per revolution is small compared to its total energy, the second term in Eq. 2.1.4 is small compared to the first one and can be neglected. For a circular motion,

$$\left(\frac{d\vec{p}}{dt}\right)^2 = \omega_o^2 \cdot p^2 \qquad (2.1.9)$$

With Eq. 2.1.9 and $p = \beta \cdot E/c$, Eq. 2.1.4 changes to

$$P = \frac{2}{3} \cdot \frac{e^2c}{R^2} \cdot \beta^4 \cdot \left(\frac{E}{mc^2}\right)^4 \qquad (2.1.10)$$

R is the radius of curvature of the circular orbit. The main message from this very important result is threefold:

(i) Only electrons and positrons are of practical value for the production of SR because of their small rest energy.

(ii) The total instantaneous power increases with the 4^{th} power of the energy of the particles which is completely different from the non relativistic case.

(iii) In contrast to linear accelerators, the instantaneous power emitted by the particles cannot be neglected in circular accelerators.

The latter point can be illustrated calculating the energy loss, δE, of an electron per revolution.

$$\delta E = P \cdot \frac{2\pi R}{c \cdot \beta} = \frac{4\pi}{3} \frac{e^2}{R} \cdot \beta^3 \cdot \gamma^4 \qquad (2.1.11)$$

$$\delta E(\mathrm{MeV}) = 8.85 \cdot 10^{-2} \cdot \frac{[E(\mathrm{GeV})]^4}{R(\mathrm{m})}$$

For a synchrotron of 6 GeV and R $\approx$ 30 m, the energy loss per each circulating electron is approximately δE = 4 MeV/revolution.

2.2 Angular distribution

The angular distribution of the instantaneous power radiated by an accelerated non-relativistic electron shows the well known $\sin^2\theta$ behaviour [48]

$$\frac{dP}{d\Omega} = \frac{e^2}{4\pi c^3} \left(\frac{d\vec{v}}{dt}\right)^2 \cdot \sin^2\theta \qquad (2.2.1)$$

The upper part of Fig. 1 illustrates the distribution. θ is the angle measured from the direction of acceleration. The length of the arrows is a measure for the instantaneous power emitted into the unit of solid angle under an angle θ. The pattern has rotational symmetry with respect to the direction of acceleration. An integration of Eq. 2.2.1 leads to the Larmor formula, Eq. 1.1.

For non-relativistic electrons, Eq. 2.2.1 holds for linear acceleration ($\vec{v} \parallel \dot{\vec{v}}$) as well as circular acceleration ($\vec{v} \perp \dot{\vec{v}}$). The radiation pattern changes completely when the electron is moving with $v \approx c$. The angular distribution of radiation is tipped forward into a narrow cone. The width of the cone can be estimated from Eq. 2.2.1. For synchrotron radiation only the case of $\vec{v} \perp \dot{\vec{v}}$ is relevant. Therefore we transform the angle $\theta_{CMS} = \pi/2 - \theta$ (see Fig. 1) from the rest frame of the moving particle to the laboratory system by [49]

$$\tan\theta_L = \frac{1}{\gamma} \cdot \frac{\sin\theta_{CMS}}{\beta + \cos\theta_{CMS}} \qquad (2.2.2)$$

A transformation of $\theta_{CMS} = \pi/2$ yields $\tan\theta_L \approx 1/\gamma$ ($\beta \approx 1$). The radiation pattern of a relativistic electron with $\gamma \gg 1$ is narrowed into a cone with an opening angle of

$$\theta_L \approx \frac{mc^2}{E} = \gamma^{-1} \qquad (2.2.3)$$

For 5 GeV electrons, θ_L is about 10^{-4} rad.

For relativistic electrons moving on a circle the radiation pattern not only depends on the transformation from the rest frame to the laboratory system but also from the specific spatial relationship between $\vec{v}$ and $\dot{\vec{v}}$ [48]. For ultra relativistic particles the relativistic effects arising from the transformation dominate the whole angular distribution.
The correct expression for the angular distribution of the total power of circulating relativistic electrons is given by [48]

$$\frac{dP}{d\Omega} = \frac{e^2}{4\pi c^3} \cdot \frac{|\dot{\vec{v}}|^2}{(1-\beta\cdot\cos\theta)^3} \cdot \left[1 - \frac{\sin^2\theta\cos^2\phi}{\gamma^2(1-\beta\cos\theta)^2}\right] \qquad (2.2.4)$$

Here the coordinates are the following: $\dot{\vec{v}}$ is in x-direction, $\vec{v}$ in z-direction (the orbit of the electron is therefore in the x/z plane). θ and ϕ are the customary polar angles defining the direction of observation. For $\gamma \gg 1$ (which is the case in most storage rings and synchrotrons), Eq. 2.2.4 reduces to

$$\frac{dP}{d\Omega} = \frac{2e^2}{\pi c^3} \cdot \gamma^6 \cdot \frac{|\dot{\vec{v}}|^2}{(1+\gamma^2\theta^2)^3} \cdot \left[1 + \frac{4\gamma^2\theta^2\cos^2\phi}{(1+\gamma^2\theta^2)^2}\right] \qquad (2.2.5)$$

The high degree of collimation is described by the factor $(1+\gamma^2\theta^2)^{-3} \approx (\gamma\theta)^{-6}$ for $\theta \gg \gamma^{-1}$.

From Eq. 2.2.5 we expect that part of the instantaneous power is radiated to the opposite of the radiation cone. This part of radiation is only $\sim(\gamma\theta)^{-6}$ times the instantaneous power radiated under $\theta \approx 0$. With $\gamma = 10^4$ (corresponding to an energy of 5 GeV), the "backward power" is only $\sim 10^{-27}$ of the "forward power".

The circulating electron radiates at any point of the orbit. Therefore the whole orbit is dressed by radiation. The high degree of collimation of this radiation is only observable in the vertical direction.

2.3. Frequency distribution

Intuitively we expect that the frequency distribution of SR extends from the fundamental frequency, $\omega_o = v/R$ of the circulating electrons, to very high harmonics. The order of magnitude of the high frequency limit can be obtained from calculating the length of a light pulse which is measured by a fixed observer in the laboratory. θ may be the angle of collimation of radiation emitted from a distinct point of the orbit. From Fig. 2 it is obvious that the observer receives light from all points of the orbit between A and B (5o). The length of the light pulse measured by the observer is equal to the difference between the transit time of the electron and light from point A to point B.

$$\Delta t = \frac{R\cdot\theta}{v} - \frac{R\cdot\theta}{c}$$

$$= \frac{1-\beta}{v} \cdot R\cdot\theta \qquad (2.3.1)$$

With $\theta \approx \gamma^{-1}$, $v/R = \omega_o$ (fundamental frequency) and $(1-\beta) = (1+\beta)^{-1} \cdot \gamma^{-2} \approx 1/(2\cdot\gamma^2)$ we obtain

$$\Delta t = \frac{1}{2} \cdot \frac{1}{\omega_o} \cdot \frac{1}{\gamma^3} \qquad (2.3.2)$$

A Fourier analysis of a light pulse of the length Δt shows that the light pulse must contain frequencies up to $1/\Delta t$. Neglecting factors of 2 we obtain from 2.3.2 for the high frequency cut off ω_c

$$\frac{\omega_c}{\omega_o} \approx \gamma^3 \qquad (2.3.3)$$

For a synchrotron like DESY ($\omega_o \approx 1$ MHz, $\gamma \approx 10^4$), the high frequency cut off is of the order of magnitude of 10^{18} Hz. This corresponds to a wave-length, $\lambda_c \approx 10^{-2}$Å. λ_c is called the "critical wavelength".

Now the question arises whether the high frequency harmonics can be resolved or not. Apart from the experimental problem, there are arguments that we have a continuous spectrum at high harmonics. Our assumption up to now was an electron travelling along a circle with an exact radius, R. In general, we have a small spread in the radius of the orbit because the electrons in an accelerator undergo betatron-oscillations. The spread in R is typically of the order of magnitude of $\Delta R/R \approx 10^{-4}$.
Therefore we do not have an ideally sharp fundamental frequency but a finite band width of the order of magnitude of $\Delta\omega_o/\omega_o \approx 10^{-4}$. In other words, from the 10^4th harmonic, the spectrum is smeared out to a continuum.

2.4 Polarization properties

The polarization properties of SR can be qualitatively explained by the pattern of electric lines of force of the radiating electron in its CMS (34). Here the electric lines of force follow the well known pattern of an electric dipole. In Fig. 3, in the upper right part, electric field vectors of an electric dipole are shown. The length of the vectors qualitatively indicates the intensity of light emitted into the corresponding direction. The pattern has rotational symmetry relative to the direction of $d\vec{v}/dt$.

An observer looking along a tangent to the circular orbit of the electron does not measure the same pattern but its transformation to the laboratory system. This is scetched qualitatively in the lower left part of Fig. 3. Due to the forward focusing of radiation the electric field vectors are nearly lying in the synchrotron plane. The polarization is complete in the synchrotron plane itself. It gradually decreases with increasing elevation angle upwards and downwards the synchrotron plane. Because of the high degree of collimation, the angular dependence of polarization has no big influence. The angular integrated intensity has still a high degree of polarization ($\sim 75\%$) (34).

For an observer within the synchrotron plane the source of radiation can be regarded as one single electric dipole emitting linearly polarized light. Observing the source point from above or below the synchrotron plane, the source of radiation can be regarded as a superposition of two electric dipoles perpendicular one to each other. Therefore, the observed radiation above and below the synchrotron plane is elliptically polarized.

2.5 Time structure

Whereas the properties of SR discussed so far are "intrinsic" properties, the time structure is a property forced upon the radiation by the mode of operation of the accelerator. It turns out that time structures can be realized which are unique in the VUV region.

2.5.1 Time structure of SR from a storage ring. Up to now we have discussed the radiative properties of one single electron in a circular orbit. In a realistic synchrotron or storage ring, however, $\sim 10^{10}$ ... 10^{15} electrons are stored. The resulting time structure of SR can be understood in the following way.

a) We suppose that the storage ring is filled continuously with electrons. Then the power would be radiated continuously in time. This mode of operation is not possible for the following reason. Due to the radiation losses, the electrons must be accelerated again and again by a RF-cavity. Only such electrons can be accelerated which have the proper phase relation to the RF. All other electrons are lost in the storage ring. The time structure therefore is closely related to the RF frequency.

b) We suppose, the RF has the same frequency as the fundamental frequency of the orbiting electrons. Then only those electrons which are collected in one single part of the orbit can be in proper phase with the RF. The length of this "bunch" of electrons is roughly a small fraction of the wavelength of the RF ($\ell \approx 1/10\ \lambda_{RF}$). The time structure due to such a mode of operation is characterized by light pulses of a length of $\tau = \ell / c$ with a repetition frequency equal to the fundamental frequency of the orbiting electrons ($\omega_0 / 2\pi$).

c) The RF may have a frequency which is a high harmonic (N) of the fundamental frequency of the orbiting electrons. Then the arguments of b) still hold with the following modifications: the bunches are shortened due to the shortening of λ_{RF}. Not only one bunch, but N bunches can fulfill the proper phase relation. Realistic values of the storage ring DORIS in Hamburg are:

RF-frequency = 480 x fundamental frequency
bunch length = 3 ... 5 cm $\hat{=}$ 0.15 ns.
Repetition frequency = $N \cdot \frac{\omega_0}{2\pi}$ = 480 MHz
This corresponds to a time distance between two bunches of 2 ns.

The situation is illustrated in Fig. 4. Not all the possible sites along the orbit must be filled with electrons. E.g., a long time, at DORIS only each 4^{th} bunch was really filled. This is called bunch occupation number 4. Also single bunch operation (like at SPEAR) is possible.

The single bunch mode of a big storage ring like DORIS or SPEAR offers an excellent time structure for a lot of experiments light pulses with a full width half maximum of ~.1 to~.2 ns and a repetition rate of 10^6 sec^{-1}. Moreover, the repetition rate has the accuracy of a quartz clock and the relative intensity distribution of the light pulse is extremely stable. These properties hold for the whole spectral range of SR and are therefore unique among all sources.

2.5.2 Time structure of SR from a synchrotron. The time structure of SR from a synchrotron is much more complicated than with a storage ring. In a synchrotron we start with "low energy" electrons from a linear accelerator (e.g. 40 MeV with Linac I at DESY). Within the synchrotron, the electrons are accelerated to their final energy. Synchronous to the increase in energy, the magnetic field of the bending magnets must be increased. Herefore, the magnets are included in oscillatory circuits with an eigenfrequency equal to the frequency of the electric mains (at DESY 50 Hz). In order to have only one direction of the magnetic field in the bending magnets, a constant fieldstrength is superimposed to the alternating field. In this way, during half (10 ms) of the period (20 ms $\hat{=}$ 50 Hz) of the magnetic field electrons can be accelerated.

The energy of the electrons follows the relation

$$E(t) = E_m \cdot \sin^2 (\pi \cdot t/2T) \qquad (2.5.1)$$

E_m means the maximum energy, and T the time of acceleration.

The time structure of SR from a synchrotron therefore contains periods of light ($\lesssim$ 10 ms at DESY) followed by periods of darkness ($\sim$10 ms). The length of light pulses is different for different wavelengths. Whereas long wavelengths are already radiated at the beginning of the acceleration period, the short wavelength spectrum around the critical wavelength is only emitted at the end of the acceleration period.

The 10 ms light pulses of SR of a synchrotron have an internal time structure like a storage ring for similar reasons as given in sec. 2.5.1. For technical reasons, not all bunches are occupied. At DESY, only 75% of the possible bunches are filled.

3. RESULTS OF THE QUANTITATIVE THEORY

In the preceeding Sections, the basic properties of SR have been discussed qualitatively. It turns out that the quantitative theory of SR confirms the qualitative results. In this Section we give the results of the quantitative calculations of Schwinger (14-16).

3.1 Angular and wavelength distribution of SR

The instantaneous power radiated by one single electron along the whole orbit per revolution in the direction ψ (angle measured from the synchrotron plane) with wavelength λ, $P(\lambda,\psi)d\lambda\, d\psi$, is given by Schwinger by ($\beta = 1$)

$$P(\lambda,\psi) = \frac{27}{32\pi^3}\cdot\frac{e^2c}{R^3}\left(\frac{\lambda_c}{\lambda}\right)^4\cdot\gamma^8\cdot\left[1+(\gamma\psi)^2\right]^2\cdot \left\{K^2_{2/3}(\xi)+\frac{(\gamma\psi)^2}{1+(\gamma\psi)^2}K^2_{1/3}(\xi)\right\} \qquad (3.1.1)$$

Here R, γ have the same meaning as in Sec. 2. λ_c is the critical wavelength, which differs only,

$$\lambda_c = \frac{4\pi}{3}\cdot R\cdot\gamma^{-3},\quad \omega_c = \frac{3}{2}\,\frac{c}{R}\cdot\gamma^3 \qquad (3.1.2)$$

by a factor of the order of magnitude of 1 from the expression already deduced in Sec. 2.3. The numerical values for λ_c are obtained from

$$\lambda_c(\text{Å}) = 5.59\ R(\text{meters})\cdot\left[E(\text{GeV})\right]^{-3} \qquad (3.1.3)$$

The K's in Eq. 3.1.1 mean modified Bessel functions with argument

$$\xi = \frac{\lambda_c}{2\lambda}\cdot\left[1+(\gamma\psi)^2\right]^{3/2} \qquad (3.1.4)$$

The quantity $P(\lambda,\psi)$ is measured in erg/(sec. Å · sterad · electron). As an example we show the angular distribution of SR (Fig. 5). In this case λ is used as a parameter. With Fig. 5 it is demonstrated that the collimation of SR depends on the wavelength of SR. For $\lambda \ll \lambda_c$ it is collimated into an angle smaller than γ^{-1}, for $\lambda \gg \lambda_c$ it is spread over an angle greater than γ^{-1}.

3.2 Polarization of SR

The angular and wavelength distribution of SR described by Eq. 3.1.1 contains two contributions in the second bracket. The first one describes the light polarized parallel to the plane of the electron orbit, the second one describes the light polarized perpendicular to the plane (51). With $\psi = 0$, the second term vanishes, and the qualitative result of Sec. 2.4 is verified: within the plane of the orbit, SR is completely polarized. Following the definition of the degree of polarization

$$\Pi = \frac{P_\parallel - P_\perp}{P_\parallel + P_\perp} \qquad (3.2.1)$$

we obtain

$$\Pi(\lambda,\psi) = \frac{K^2_{2/3} - \frac{(\gamma\psi)^2}{1+(\gamma\psi)^2}K^2_{1/3}}{K^2_{2/3} + \frac{(\gamma\psi)^2}{1+(\gamma\psi)^2}K^2_{1/3}} \qquad (3.2.2)$$

In Fig. 6, the degree of polarization is shown as a function of the elevation angle ψ. The wavelength is used as a parameter. The calculation has been done for DESY (E = 6 GeV, R = 31.7 meters).

3.3 Spectral distribution of SR

Eq. 3.1.1 can be integrated over the elevation angle ψ. Then we obtain the instantaneous power, radiated by one electron per revolution into the whole solid angle, as a function of wavelength: $P(\lambda)d\lambda$ with

$$P(\lambda) = \frac{3^{5/2}}{16\pi^2}\cdot\frac{e^2\cdot c}{R^3}\cdot\gamma^7\cdot\left(\frac{\lambda_c}{\lambda}\right)^3\cdot\int_{\lambda_c/\lambda}^{\infty} K_{5/3}(\eta)\,d\eta \qquad (3.3.1)$$

$P(\lambda)d\lambda$ is the spectral distribution of SR. It contains a universal function (λ_c/λ-dependent part). In a double logarithmic picture, with a variation of the energy of the electron, the curve must be shifted with the third power to the left (due to the factor $\lambda_c/\lambda \sim \gamma^{-3}$) and with the seventh power upwards (due to γ^7). Fig. 7 shows the spectral distribution of SR for different energies of the electrons and for R = 31.7 m (DESY). The spectra

have their maxima at $\lambda = 0.42\ \lambda_c$. They fall off exponentially for $\lambda \ll 0.42\lambda_c$ and decrease slowly for $\lambda \gg \lambda_c$.

The asymptotic behavior of Eq. 3.3.1 yields for $\lambda \gg \lambda_c$

$$P\left[\frac{\text{erg}}{\text{sec}\cdot\text{Å}\cdot\text{electron}}\right] \approx 90\cdot\left[R(\text{meters})\right]^{-2/3}\cdot\left[\lambda(\text{Å})\right]^{-7/3} \qquad (3.3.2)$$

The power radiated with $\lambda \gg \lambda_c$ is nearly independent of the energy of the electrons.

3.4 Total angular distribution

Wavelength integration of Eq. 3.1.1 leads to the total angular distribution $P(\psi)d\psi$ with

$$P(\psi) = \frac{e^2\cdot c}{R^2}\cdot\gamma^5\cdot\left[1+(\gamma\psi)^2\right]^{-5/2}\cdot\left[\frac{7}{16}+\frac{5}{16}\cdot\frac{(\gamma\psi)^2}{1+(\gamma\psi)^2}\right] \qquad (3.4.1)$$

The angular distribution contains two contributions in the second bracket. One of them describes the light polarized parallel to the synchrotron plane. The other one (ψ-dependent) describes the SR polarized perpendicular to the synchrotron plane [51]. An angular integration of both contributions separately shows that the integrated intensity has a degree of polarization of 75%. This result is independent of the radius of the orbit and the energy of the electrons. As can be seen from Fig. 6, the polarization is much higher if we restrict ourselves to small elevation angles. The tolerable angles for a certain degree of polarization depend on the wavelength of SR.

3.5 Total power

Integration of Eq. 3.1.1 over λ and ψ leads to the instantaneous total power radiated by one single electron along one revolution.

We get

$$P = \frac{4\pi}{3}\cdot\frac{e^2}{R}\cdot\gamma^4 \qquad (3.5.1)$$

The same result is also obtained from Eq. 2.1.10 if P is integrated over one revolution (multiplication with $2\pi\cdot R/c$).

4. MODIFICATION OF THE THEORY OF SR FOR REALISTIC SOURCES

The theoretical results discussed in Sec. 3 are only valid for one single monoenergetic electron. In realistic synchrotrons and storage rings we must take into account:

(i) Not only one but 10^{10} to 10^{15} electrons are stored in the orbit.

(ii) In synchrotrons, the electrons are not monoenergetic but are accelerated from low to high energies during a period of acceleration.

(iii) The geometry is different from the assumption in Sec. 3. In realistic synchrotrons and storage rings, straight parts are included in the orbit of the electrons. In the straight parts the electrons do not radiate.

4.1 Synchrotron radiation of a group of electrons

If many electrons are present in one bunch, apart from the RF-range; the emitted power is

$$P(\text{N electrons}) = N\cdot P(\text{single electron}) \qquad (4.1.1)$$

This is straight forward as long as coherence effects can be neglected.

McMillan [52], Schiff [53], and Nodvick and Saxon [54] have shown that SR of a group of electrons is a superposition of an incoherent and a coherent part. Coherence effects only occur if the electrons have a stable distribution within the bunch. If the angular coordinate of the k th electron, $\varphi_k + \omega_o\cdot t$, is well defined, than the contribution of the k th electron to the nth harmonic of the radiation field contains a phase factor $\exp(-in\varphi_k)$ which is responsible for coherence effects. It has been shown that the coherent

part of SR is independent of the wavelength of SR and can be neglected completely in the shorter wavelength region of SR It gets important only in the very long wavelength region ($\sim$ RF-frequencies) where the incoherent part of radiation is very small. For a uniform distribution of N electrons within an angular interval α, the coherent part of the total power is given by (54)

$$P_{coh} = (N^2 \cdot \omega_o \cdot e^2/R) \cdot (\sqrt{3}/\alpha)^{4/3} \qquad (4.1.2)$$

R is the radius of curvature, ω_o the fundamental frequency. For practical purposes in the field of spectroscopy with SR, Eq. 4.1.1 can always be used.

4.2 SR of electrons which are not monoenergetic

In Sec. 2.5.2 it has been pointed out that in synchrotrons the electrons are accelerated from very low to high energies. The time-dependence of the energy of the electrons at DESY is given by Eq. 2.5.1. This Eq. must be put into the results of Schwinger for monoenergetic electrons and the time average must be calculated. The angular and wavelength distribution $P(\lambda, \psi)$ of Eq. 3.1.1 changes to

$$\bar{P}(\lambda, \psi, E_m) = \frac{1}{T} \int_0^T P(\lambda, \psi, E(t))dt \qquad (4.2.1)$$

In a similar way all the results of Sec. 3 must be modified. More details are given by Tomboulian and Hartmann (25) for $E(t) = E_m \cdot \sin(\pi t/2T)$ and by Tomboulian and Bedo (26) for $E(t) = E_m \cdot \sin^2(\pi t/2T)$. In storage rings, the results of Schwinger can be used without this modification. They must only be multiplied with the total number of electrons stored.

4.3 Geometrical effects

In realistic synchrotrons and storage rings, straight sections are included in the orbit. Therefore the geometrical radius of an accelerator is larger than the "magnetic" radius of the bending magnets. In the results of Sec. 3, always the "magnetic" radius must be used. The time required for one revolution is longer than the time of radiation by a factor R_{geom}/R_{mag}. Therefore the results of Sec. 3 must be multiplied by R_{mag}/R_{geom}.

The influence of geometry can be included in the theoretical results normalizing the radiated power to the current in the accelerator instead of the number of electrons.

4.4 Intensity available for the experiments

For practical purposes it is useful to know the number of photons of energy $\hbar\omega$ per energy interval 1 eV per second which are accepted by the experiment. Therefore, $P(\lambda, \psi)d\lambda\, d\psi$ (Eq.3.1.1) must be changed to $P(\hbar\omega, \psi)d(\hbar\omega)d\psi$.

In many cases nearly all photons are accepted within a certain horizontal angular interval independent from the elevation angle. Then we start from $P(\lambda)d\lambda$ (Eq. 3.3.1) which is transformed to $P(\hbar\omega)d(\hbar\omega)$. In both cases, the horizontal angular acceptance, $d\alpha$, is taken into account by a factor of $d\alpha/2\pi$ (Eq. 3.1.1 and 3.3.1 hold for the total horizontal angle, 2π).

The asymptotic behavior of Eq. 3.3.1 for $\lambda \gg \lambda_c$ was given by Eq. 3.3.2. It is useful to change Eq. 3.3.2. We obtain (55)

$$N = 4.5 \times 10^{12} \cdot j \cdot R^{1/3} \cdot (\hbar\omega)^{-2/3} \qquad (4.4.1)$$

N denotes the number of photons per sec per eV per mA in an infinitely high slice of one mrad horizontal width. j is the current (in mA), R the bending radius (in m) and $\hbar\omega$ is the photon energy (in eV). Eq. 4.4.1 only holds for $\hbar\omega \ll \hbar\omega_c$.

To give an impression of realistic numbers of photons, in Fig. 8 some calculations for DESY and DORIS are shown. They give the number of photons per eV per sec into a window of 2 x 2 cm^2, 40 m away from the source point, as a function of photon energy.

Acknowledgement

The authors are grateful to the members of the SR-group at DESY, especially to U. Hahn, for helpful discussions.

References

1. G.C. Baldwin, Physics Today 28, 9 (1975)
2. J. Larmor, Phil.Mag. 44, 503 (1897)
3. A. Liénard, L'Eclairage Elec. 16, 5 (1898)
4. G.A. Schott, Ann.Phys. 24, 635 (1907) and Electromagnetic Radiation, Cambridge University Press, Cambridge (1912)
5. D. Iwanenko and J. Pomeranchuk, Phys.Rev. 65, 343 (1944)
6. J.P. Blewett, Phys.Rev. 69, 87 (1946)
7. F.R. Elder, A.M. Gurewitsch, R.V. Langmuir, and H.C. Pollock, Phys.Rev. 71, 829 (1947)
8. D. Ivanenko and A.A. Sokolov, Doklady Akad. Nauck 59, 1551 (1948)
9. A.A. Sokolov, N.P. Klepitov and J.M. Ternov, Doklady Nauk SSSR 89, 665 (1953)
10. A.A. Sokolov and J.M. Ternov, Sov.Phys. JETP 1, 227 (1955)
11. A.A. Sokolov and J.M. Ternov, Sov.Phys. JETP 4, 396 (1957)
12. A.A. Sokolov and J.M. Ternov, Sov.Phys. Doklady 8, 1203 (1964)
13. A.A. Sokolov and J.M. Ternov, Synchrotron Radiation, Pergamon Press 1968
14. J. Schwinger, Phys.Rev. 70, 798 (1946)
15. J. Schwinger, Phys.Rev. 75, 1912 (1949)
16. J. Schwinger, Proc.Nat.Acad.Sci. U.S. 40, 132 (1954)
17. H. Olsen, Det Kgl.Norske Videnskabers Selskabs Skrifter Nr. 5 (1952)
18. M. Neumann, Phys.Rev. 90, 682 (1963)
19. F.R. Elder, R.V. Langmuir, and H.C. Pollock, Phys.Rev. 74, 52 (1948)
20. I.M. Ado and P.A. Cherenkov, Sov.Phys. Doklady 1, 517 (1956)
21. F.A. Korolev, O.F. Kulikov, and A.S. Yarov, Sov.Phys. JETP 43, 1653 (1953)
22. F.A. Korolev and O.F. Kulikov, Opt.Spectr. 8, 1 (1960)
23. D.A. Corson, Phys.Rev. 86, 1052 (1952), and Phys.Rev. 90, 748 (1953)

24. D.H. Tomboulian, U.S. Atom, En.Comm. NP-5803 (1955)
25. D.H. Tomboulian and P.L. Hartman, Phys.Rev. 102, 1423 (1956)
26. D.H. Tomboulian and D.E. Bedo, J.Appl.Phys. 29, 804 (1958)
27. P. Joos, Phys.Rev. Letters 4, 558 (1960)
28. D.E. Bedo, D.H. Tomboulian, and J.A. Rigert, J.Appl.Phys. 31, 2289 (1960)
29. R.P. Madden and K. Codling, Phys.Rev.Letters 10, 516 (1963)
30. R.P. Madden and K. Codling, Phys.Rev.Letters 12, 106 (1964)
31. R.P. Madden and K. Codling, JOSA 54, 268 (1964) J.Appl.Phys. 36, 830 (1965)
32. G. Bathov, E. Freytag and R. Haensel, J.Appl.Phys. 37, 3449 (1966)
33. R. Haensel and C. Kunz, Z.Angew.Phys. 23, 276 (1967)
34. R.P. Godwin, in Springer Tracts in Modern Physics 51, 1 (1969), ed. by G. Höhler, Springer/Berlin, Heidelberg, New York
35. W. Hayes, Contemp.Physics 13, 441 (1972)
36. K. Codling, Rep.Progr.Phys. 36, 541 (1973)
37. F.C. Brown, Solid State Physics Vol. 29, ed. by F. Seitz, D. Turnbull and H. Ehrenreich, Academic Press, New York 1974
38. R.P. Madden, in X-ray Spectroscopy, ed. by L.V. Azaroff, Mc Graw Hill 1974
39. R. Haensel, in Festkörperprobleme (Advances in Solid State Physics) XV, ed. by H.J. Queisser (Pergamon Vieweg, Braunschweig 1975)
40. C. Kunz, in Optical Properties of Solids - New Developments, ed. by B.O. Seraphin, North Holland, Amsterdam (1976)
41. B. Sonntag, in Rare Gas Solids II, ed. by M.L. Klein and J.A. Venables, Academic Press (1976)
42. E.E. Koch, C. Kunz, and B. Sonntag, Rep.Progr. in Physics (to be published)
43. Proc. First Intern. Conference Vac. UV Rad. Phys., ed. by G.L. Weissler, J.Quant.Spectrosc. Radiat. Transfer 2, 313 (1962)
44. Proc.Intern.Symp. for Synchr.Rad.Users, ed. by G.V. Marr and I.H. Munro, Daresbury Nuclear Phys.Lab. DNPL/R26 (1973)

45. Research Applications of Synchrotron Radiation, ed. by R.E. Watson, M.L. Perlman, Brookhaven National Lab. BNL 50381 (1973)

46. Proc. IVth Intern.Conference on VUV Rad.Physics, Hamburg 1974, ed. by E.E. Koch, R. Haensel, and C. Kunz, Pergamon Vieweg, Braunschweig 1974

47. G.V. Marr, I.M. Munro and J.C.C. Sharp, DNPL/R24 (1972) and Supplement DL/TN 127 (1974)

48. A detailed discussion of the radiation of moving charges including electrons in a synchrotron, is given, e.g. in J.D. Jackson, Classical Electrodynamics, Wiley, New York

49. This kind of argumentation has been given by R.P. Godwin, Ref. 34

50. See, e.g. A. Sommerfeld, Elektrodynamik, Akademische Verlagsgesellschaft Geest & Portig K.G. Leipzig 1964, p. 239

51. K.C. Westfold, Astrophys. J. 130, 231 (1959)

52. E.M. McMillan, Phys.Rev. 68, 144 (1945)

53. L.I. Schiff, Rev.Sci.Instr. 17, 6 (1946)

54. J.S. Nodvick and D.S. Saxon, Phys.Rev. 96, 180 (1954)

55. E.E. Koch, in Interaction of radiation with condensed matter, L.A. Self (editor), publication of the Trieste Center for Theoretical Physics Int.Atomic Energy Agency, Wien 1976, chapter 19 (in press)

Figure Captions

Fig. 1 Schematic angular distribution of the instantaneous power radiated by an accelerated electron with non-relativistic and relativistic velocity (v ≪ v).

Fig. 2 Outline of the geometry for the calculation of the length of a light pulse measured by an observer in the laboratory. The arrow points to the observer who can receive light emitted along the part AB of the orbit.

Fig. 3 Dipole radiation pattern in the rest frame of a circulating relativistic electron and its appearance in the laboratory system (schematic).

Fig. 4 Time structure of SR from the storage ring DORIS.

Fig. 5 Time averaged angular distribution of SR from an electron which is accelerated from 0 to 6 GeV, R = 31.7 m (DESY). The wavelength of SR is used as a parameter. For the calculation, Eq. 2.5.1, Eq. 3.1.1 and Eq. 4.2.1 have been used.

Fig. 6 Angular dependence of the degree of polarization of SR for different wavelengths (monoenergetic electrons with 6 GeV).

Fig. 7 Time averaged spectral distribution of SR from an electron which is accelerated from 0 to E_{max}, R = 31.7 m. For the calculation, Eq. 2.5.1 and Eq. 3.3.1 have been used.

Fig. 8 Spectral distribution of SR from the synchrotron DESY and the storage ring DORIS into an aperture of 2 cm x 2 cm, 40 m away from the source point. The cut-off wavelengths are indicated by arrows. The high current of 6 A has not been realized.

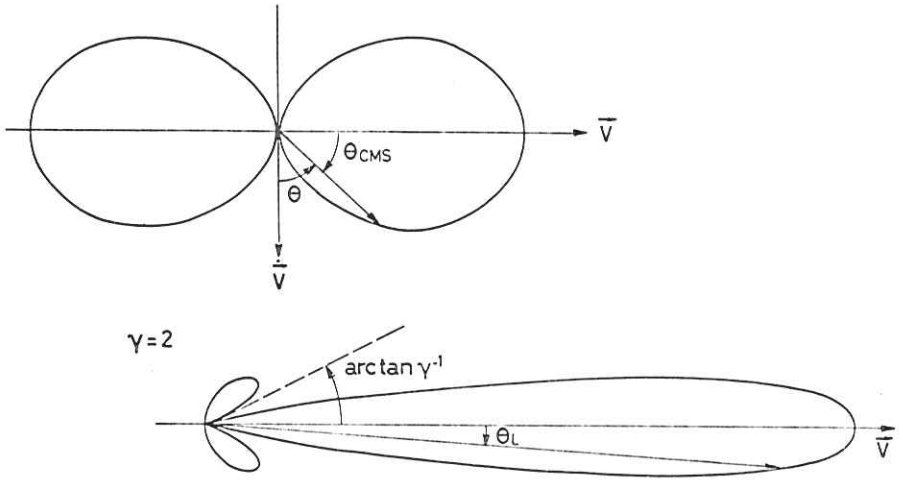

Fig. 1

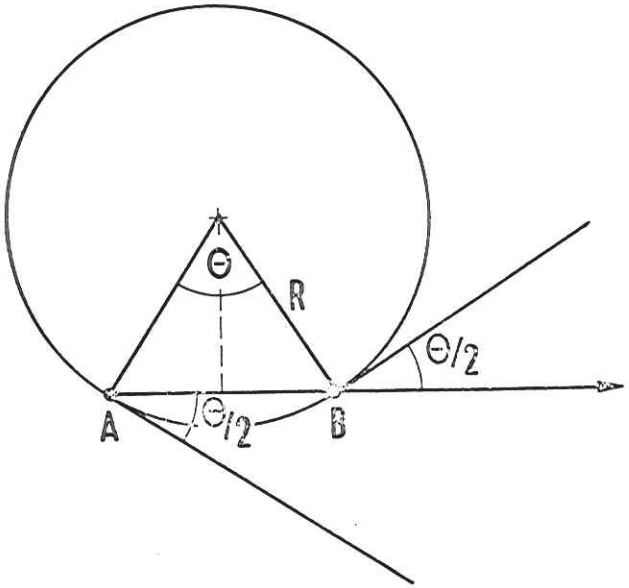

Fig. 2

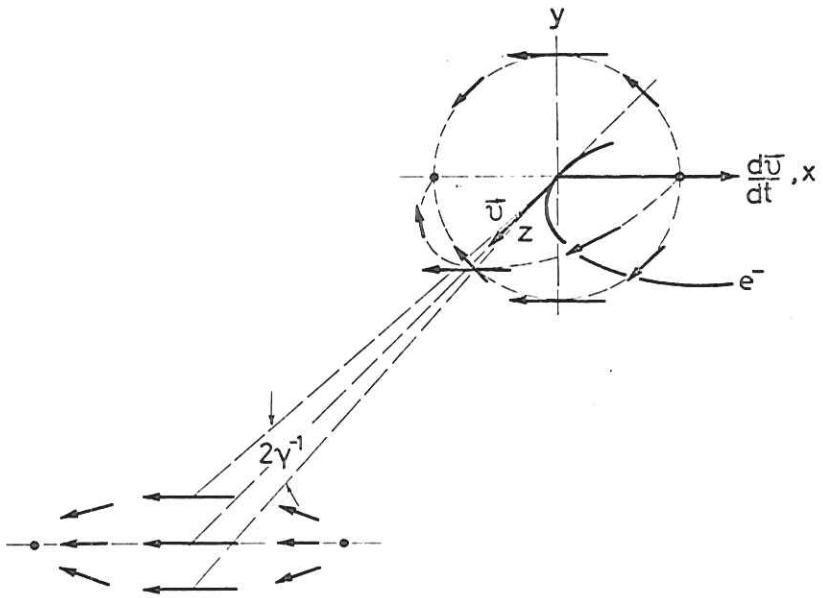

Fig. 3

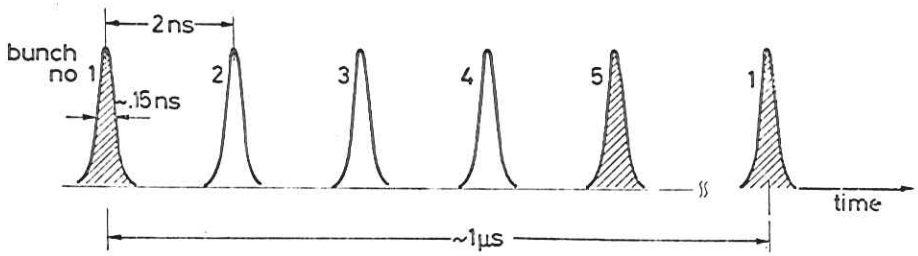

Fig. 4

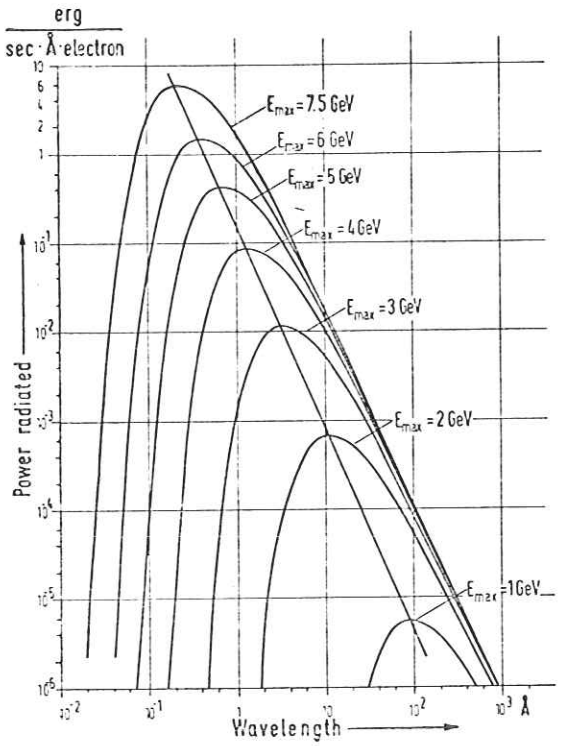

Fig. 7

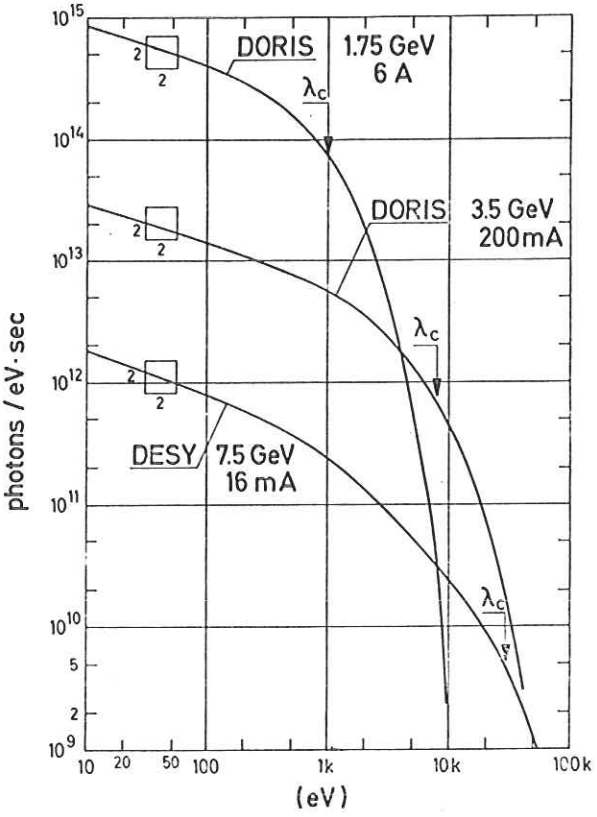

Fig. 8

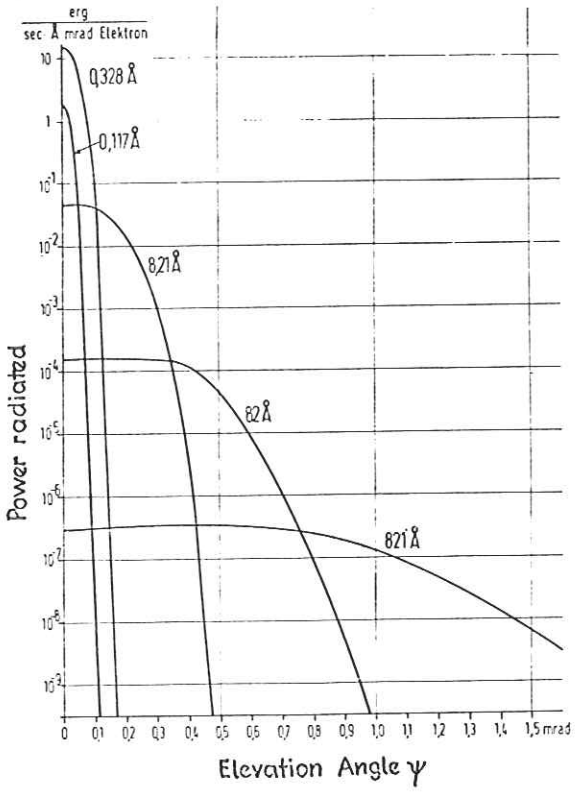

Fig. 5

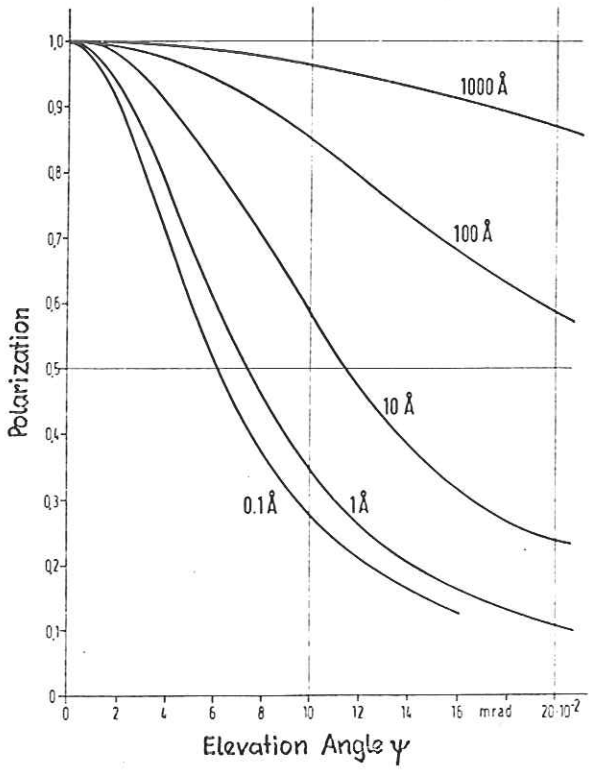

Fig. 6